

Bio-based composite reinforced with peanut shells prepared by ionizing radiation for removal of Ni²⁺ and Co²⁺ ions

Yahya H.F. Al-Qudah^a, N.R. Hegazy^b, Ghada A. Mahmoud^{b,*}, E.A. Hegazy^b

^aAl-Balqa Applied University, Hosun College, Jordan

^bNational Center for Radiation Research and Technology, Atomic Energy Authority, P.O. Box: 29, Nasr City, Cairo, Egypt, Tel. +2-01065495895; Fax: +2-022 2749298; email: ghadancrrt@yahoo.com

Received 26 September 2021; Accepted 21 January 2022

ABSTRACT

Peanut shells were incorporated in polymeric matrix of chitosan/xanthan/acrylic acid to form Cs/XN/AAC-PS composite by using gamma irradiation. It was found that 10 kGy irradiation dose is sufficient to crosslinking the network structure and increasing with irradiation dose up to 30 kGy. A decrease in gel content was observed at 40 kGy. The gel content was found to be increased with increasing AAC content. The swelling percentage decreases by increasing of AAC content and irradiation dose except at 40 kGy. Characterization the composite was performed by Fourier-transform infrared spectroscopy, field emission scanning electron microscopy, and dynamic light scattering. The adsorption performance of Cs/XN/AAC-PS composite towards the removal of Ni²⁺ and Co²⁺ was investigated. The adsorption capacity was found to be enhanced with increasing the temperature, initial metal ion concentration and pH. The highest adsorption capacity values for Ni²⁺ and Co²⁺ by Cs/XN/AAC-PS composite are 6.84 and 3.73 mmol/g at pH 6 and initial concentration 150 mg/L, respectively. The maximum capacity was done at the adsorbent dosage of 0.1 g.

Keyword: Adsorption; Composite; Metal ions removal; Chitosan; Xanthan

1. Introduction

Wastewater from many industries includes heavy metal ions. It is discharged into natural water directly and becomes dangerous to human health [1–3]. The removal of metal ions from wastewater is considering a significant target [4]. The excessive utilization of nickel causes various problems [5]. Cobalt can produce vomiting, illness, diarrhea, asthma, pneumonitis, and weight loss [6]. Heavy metal ions in wastewater can be extracted using broad techniques include solvent extraction, precipitation, vacuum, membrane, ionic exchange, and adsorption [7]. Adsorption is an important technique for managing the extent of pollution [8]. It is used to concentrate on waste streams and eliminate heavy metal ions.

Co-polymer hydrogels have high consideration as adsorbents for eliminating heavy metal ions because it can be incorporated into various functional groups into the polymeric networks [9,10]. Chitosan has desirable properties for the adsorption of metal ions. It has the amino groups (–NH₂) that can combine with metal ions [11]. Xanthan gum is anionic heteropolysaccharide. It contains –OH and –COOH groups that have excellent adsorption properties [12]. The presence of synthetic polymer with a natural one in the hydrogel produces an adsorbent that has synergetic properties [13].

The use of low-cost materials as sorbents such as agricultural wastes has been a focus on wastewater technology [14]. Agricultural wastes are ordinarily constituted of lignin and cellulose [15]. Biosorbent from agricultural wastes

* Corresponding author.

have polyfunctional groups such as $-\text{NH}_2$, $-\text{COO}^-$, $-\text{C}=\text{O}$, OH^- and PO_4^{2-} [16]. Several studies use peanut shells as an adsorbent for adsorbing of different pollutants [17,18]. Peanut shells are inexhaustible, non-edible, and renewable lignocellulosic materials resources [19]. However, it is not easy to separate the suspended solids from aqueous solution [20]. From this regard, in this study, peanut shells were incorporated in chitosan/xanthan/acrylic acid to form Cs/XN/AAC-PS composite for the first time by aiding of gamma irradiation. Ionizing radiation is an excellent technique in the fabrication of materials. The lack of chemical initiator and cross-linker produces high purity final product; it does not require further purification [21–23]. The prepared composite was used as an adsorbent for the removal of Ni^{2+} and Co^{2+} . For this purpose, the operation conditions were studied.

2. Materials and methods

2.1. Materials

Medium molecular weight chitosan (Cs) and AAC were obtained from Sigma-Aldrich Inc. and xanthan was get from Oxford Laboratory Reagent, India. Other chemicals such as NiCl_2 and CoCl_2 were purchased from El-Nasr Co. for chemical industries, Egypt. All chemicals were used as received.

2.2. Punt shells treatment

Punt shells (PS) were collected from markets and were cleaned with distilled water to remove the adhering dust. The shells were dried in air and were ground to a fine powder.

2.3. Preparation of hydrogel

3 g of chitosan (Cs) was dissolved in 100 mL distilled water, heated and stirred at 80°C for 120 min to form a homogeneous mixture. 1 g of xanthan (XN) was dissolved in 100 mL distilled water, heated and stirred at 80°C for 30 min. The solutions were mixed, and then 1 wt.% of PS and different ratios (0.5–1.5 wt.%) of acrylic acid (AAC) were supplemented and stirring for 30 min at ambient. The viscous solutions were irradiate by ^{60}Co gamma source at different irradiation doses from 10 to 40 kGy at a dose rate of 1.4 kGy/h. After irradiation, the samples were immersed in water to exclude the unreacted ingredient, then air-dried.

2.4. Instrumentation

Fourier-transform infrared spectroscopy (FTIR) spectra was recorded over the range of $400\text{--}4,000\text{ cm}^{-1}$, on Bruker, Unicomp Infrared Spectrophotometer, Germany.

Morphological study was done using field emission scanning electron microscopy (SEM) Model Quanta FEG-250 (field emission gun) with accelerating voltage 30 K.V., magnification 14x up to 1,000,000 and resolution for Gun.1n), Netherlands. The particle size was analyzed by dynamic light scattering (DLS) instrument (Zetasizer Nano Series (HT), Nano ZS, Malvern Instruments, UK).

The metal ion concentration was evaluated using Agilent 700 Series ICP Optical Emission Spectrometer (ICP-OES), Agilent Technologies Inc., USA.

2.5. Gel content

The dried weighted samples were immersed in distilled water overnight at 70°C then, cleaned with warm water to extract the soluble fraction, dehydrated to a fixed weight. The gel content was estimated using the following formula:

$$\text{Gel content (\%)} = \frac{W_d}{W_o} \times 100 \quad (1)$$

where W_d and W_o are the dried sample weights after and before extraction, respectively.

2.6. Swelling measurements

The dried weighted samples were immersed in aqueous or in buffer solutions at desirable pH (2, 4, 6, 8 and 10) for a definite time at ambient. Then, the excess water was displaced using a filter paper and re-weighed. The swelling percentage was determined as:

$$\text{Swelling (\%)} = \frac{W_s - W_d}{W_d} \times 100 \quad (2)$$

where W_s is the mass of the swollen sample and W_d is the mass of dehydrated one.

2.7. Adsorption studies

The effect of experimental controlling parameters on the adsorption of Ni^{2+} and Co^{2+} ions by Cs/XN/AAC-PS compared with Cs/XN/AAC hydrogel were studied.

Each experiment was repeated three times according to the following procedures.

2.7.1. Effect of pH

0.1 g of sorbent was placed in a volumetric tube contains 25 mL of metal ions solution of concentration 20 mg/L at suitable pH. The pH of the solution was adjusted by 0.1 mol/L of HCl or NaOH and shaken at room temperature for 24 h. The adsorption capacity q_e (mmol/g) at equilibrium was evaluated by:

$$q_e = \frac{(C_i - C_e)}{W \times A} \times V \quad (3)$$

where C_i (mg/L) is the initial metal ions concentration. C_e is the final metal ions concentration. V (L) is the solution volume. W (g) is the weight of the sample and A is the atomic weight of metal.

2.7.2. Effect of metal ion concentration

The effect of initial metal ion concentration was studied using various concentrations of metal ions ranged from

25 to 150 mg/L. 0.1 g of sorbent was placed in a volumetric tube contains 25 mL of a definite concentration of metal ions solution at pH; 6. Shaking at room temperature for 24 h. The sorption capacity was calculated using Eq. (3).

2.7.3. Effect of adsorbent dosage

The effect of the adsorbent dosage was studied using various weights of adsorbent ranged from 0.1 to 0.4 g. A definite weight of the adsorbent was putted in a volumetric tube contains 25 mL of 20 mg/L of metal ions solution at pH; 6. Shaking at room temperature for 24 h. The sorption capacity was calculated using Eq. (3).

2.7.4. Effect of temperature

0.1 g of sorbent was placed in a volumetric tube contains 25 mL of metal ions solution of concentration 20 mg/L at pH; 6. Shaking in a water bath at 25°C for 24 h. The experiment was repeated at 40°C and 60°C. The sorption capacity was calculated using Eq. (3).

To compare the validity of model equations more definitely a normalized standard deviation (%) is calculated as follows:

$$\Delta q (\%) = 100 \times \sqrt{\frac{[(q_e^{\text{exp}} - q_e^{\text{cal}}) / q_e^{\text{exp}}]^2}{N - 1}} \quad (4)$$

where the superscripts 'exp' and 'cal' show the experimental and calculated values and N is the number of measurements.

3. Results and discussion

The synthesis of composite hydrogel in aqueous medium using gamma irradiation technique preformed via radical mechanism, Fig. 1. The radiolysis of water produces hydroxyl radicals that abstracting hydrogen atoms from the polymer chains. Whatever, the macroradicals are created moreover the macroradicals produce directly on polymer chains [24]. Moreover, the radicals that formed on acrylic acid by breaking the double bond of vinyl group by the effect of gamma radiation. Thus, polymerization and cross-linking occur simultaneously to get a network structure [13].

The impact of AAc content on the gel content percentage is investigated in Fig. 2. The gel content enhances with increasing of AAc content in the network matrix. Due to improving the diffusion rate of the monomer into the bulk polymer that promotes the propagation of growing chains. According to the obtained data 10 kGy irradiation dose is sufficient to get cross-linking network structure. It can be noted that the gel content increases with increasing the irradiation dose from 10 to 30 kGy, however, a decrease in gel content was observed at raising the irradiation dose to 40 kGy. The increase of irradiation dose improves the free radicals formation that leads to a high content of gel [25,26]. However, at 40 kGy a drop in the gel content was observed that may be resulted from degradation of the polymeric network practically the system based on natural polymers [13].

The swelling of the prepared composites was investigated to know the behavior of the prepared composite in aqueous solution. The swelling property is an important character in the materials that are used as adsorbent materials. In this part, the swelling percentage of the prepared composite was investigated as a function of AAc content at different irradiation doses as represented in Fig. 3. It can be observed that the swelling percentage decreases as increasing of AAc content and irradiation dose except at 40 kGy. It must be known that the swelling ability of the polymeric matrix is proportional to the flexibility of the matrix and inversely proportional to the cross-linking structure [27,28]. From this view, it can be explained that the cross-linked structure of Cs/XN/AAc-PS enhances by increasing AAc content and irradiation dose as well as the swelling percentage decreases. However, at irradiation dose of 40 kGy the gel content decreased as mentioned above and therefore the cross-linking structure decreased. In other words, at 40 kGy the flexibility of the polymeric matrix increased as well as the swelling percentage was also increased.

FTIR spectra of Cs/XN/AAc-PS composite of different AAc content is shown in Fig. 4. Broadband appears at 3,438 cm^{-1} assigned to O–H and N–H. The stretching band of the C–H group appears at 2,928 cm^{-1} . The band at 1,718 cm^{-1} was ascribable to the C=O of the carbonyl group and amide I. A weak signal was observed at 1,543 cm^{-1} due to the N–H deformation of the amino group (amine II). The band at 1,156 cm^{-1} corresponds to the acetal group [29–32]. The increase of AAc content from 15 to 30 wt.%, the intensity of the C=O stretching band was increased and

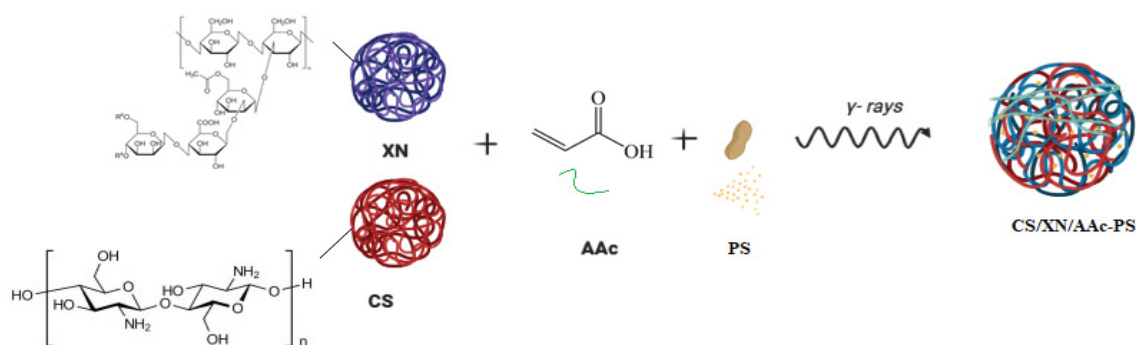


Fig. 1. Scheme represents the preparation of Cs/XN/AAc-PS composite.

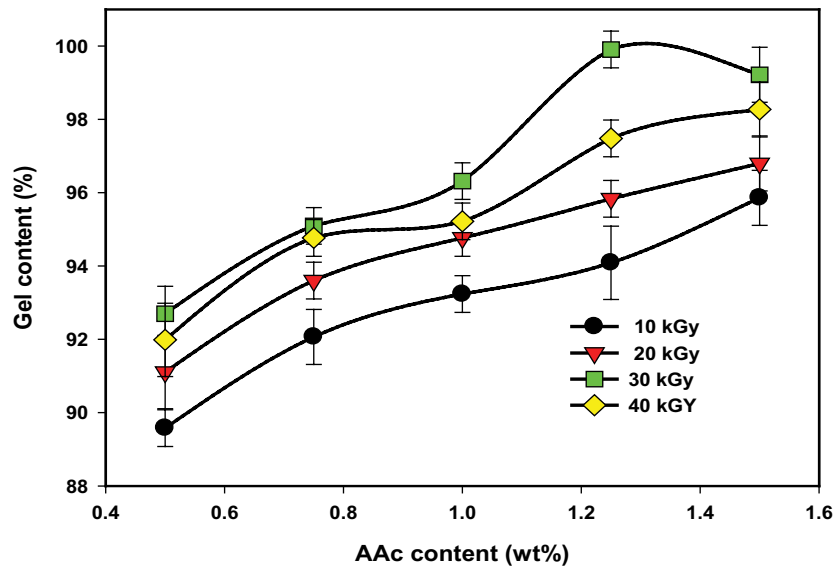


Fig. 2. The gel content at different irradiation doses as a function of the AAc content.

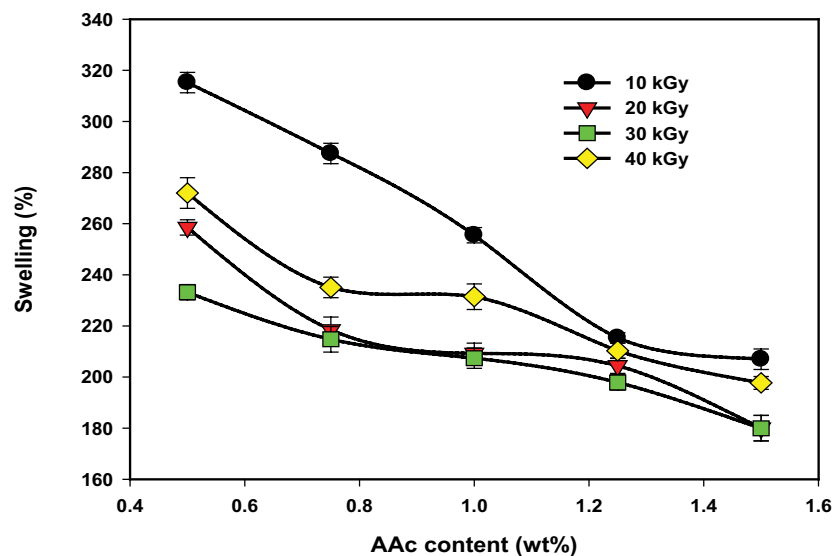


Fig. 3. The swelling percentage at different irradiation doses as a function of the AAc content.

negatively shifted to $1,709\text{ cm}^{-1}$ as a result of increasing the crosslink density. On the other hand, it can be noted that a little shortage and shifted in bands were produced because of increasing the irradiation dose from 10 to 30 kGy.

Fig. 5a shows the surface morphology of Cs/XN/AAc hydrogel by field emission scanning electron microscopy (FESEM). As seen in the figure, the surface appears as a beehive structure. The surface is turned into crushed by adding PS in Cs/XN/AAc-PS composite as observed in Fig. 5b. DLS examination for Cs/XN/AAc-PS composite (Fig. 5c) revealed that PS is ordinarily distributed and the average size is 266 nm.

3.1. Adsorption study

The adsorption performance of the prepared Cs/XN/AAc-PS composite towards the remediation of Ni^{2+} and

Co^{2+} from aqueous solutions was investigated. The effects of pH, contact time, initial concentration, the dosage of sorbent, and temperature on the adsorption have been investigated.

3.1.1. Effect of pH

The adsorption capacity dependence of Ni^{2+} and Co^{2+} on pH by Cs/XN/AAc-PS and Cs/XN/AAc sorbents is shown in Fig. 6. It was found that the adsorption capacity increases with pH increment up to pH = 6 above this value a precipitation of metal ions as metal hydroxide was done. Also, the adsorption capacity of Cs/XN/AAc-PS composite is higher than Cs/XN/AAc hydrogel due to the presence of more active groups available for adsorption by introducing PS into Cs/XN/AAc matrix. It can be noted that in a highly acidic medium the active groups ($-\text{NH}_2$, $-\text{OH}$, and $-\text{COOH}$)

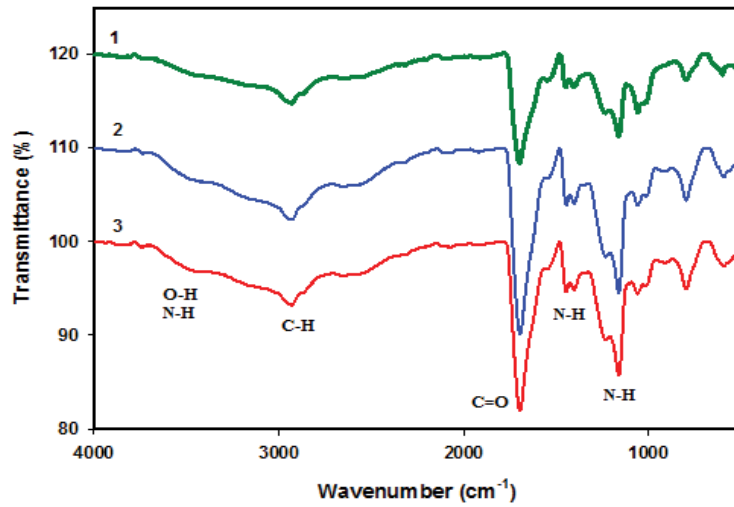


Fig. 4. FTIR spectra of Cs/XN/AAC-PS composite of AAC content (1) 15% and (2) 30% at irradiation dose 10 kGy and (3) 30% at irradiation dose 40 kGy.

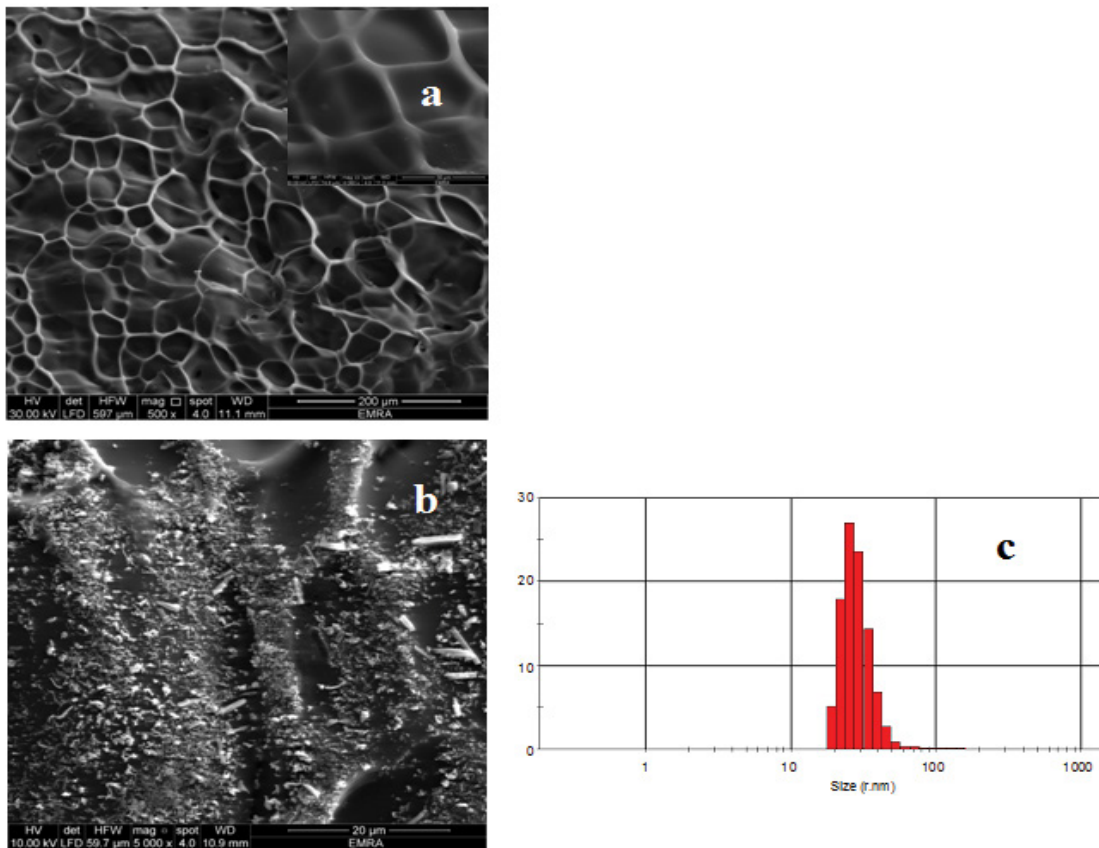


Fig. 5. FESEM images of Cs/XN/AAC (a), Cs/XN/AAC-PS (b), and DLS of Cs/XN/AAC-PS (c).

in Cs/XN/AAC-PS sorbent are protonated that restricted the interaction of Ni²⁺ and Co²⁺ with Cs/XN/AAC-PS functional groups [33]. Deprotonation of functional groups is as increase as in pH of the medium so an enhancement of Ni²⁺ and Co²⁺ ions adsorption. This is due to increasing the electrostatic interactions of the negatively charged sites and

the positively charged metal ions; Ni²⁺ and Co²⁺ ions. On the other hand, the adsorption capacity towards Ni²⁺ is higher than Co²⁺ where the highest adsorption capacity values for Ni²⁺ and Co²⁺ by Cs/XN/AAC-PS composite are 0.7200 and 0.3460 mmol/g at pH 6, respectively. The possible explanation for this result may be attributed to the hydrated

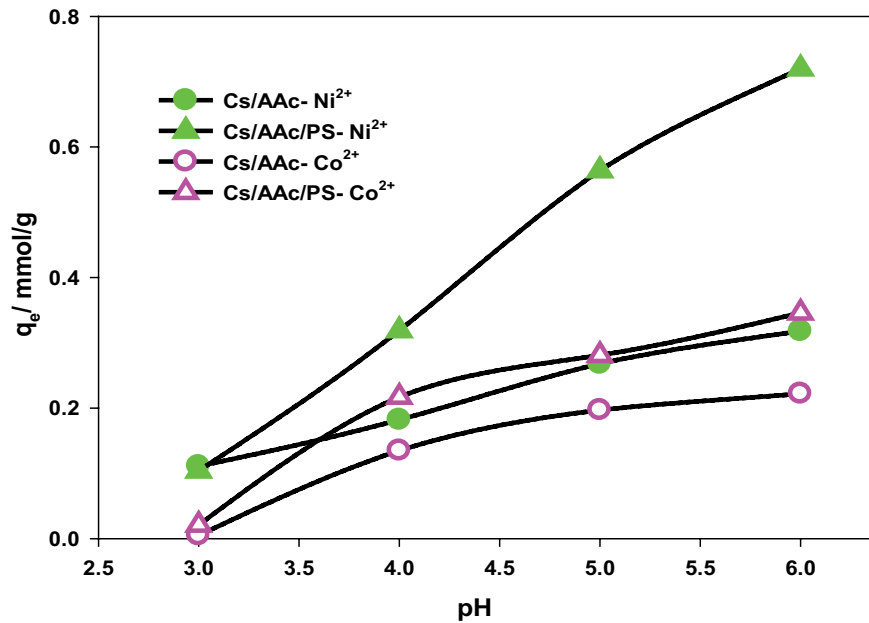


Fig. 6. Effect of pH on the adsorption capacity of Co²⁺ and Ni²⁺ by 0.1 g of Cs/AAc/PS composite compared with Cs/AAc parent hydrogel in 25 mL of initial concentration 20 mg/L at contact time 24 h.

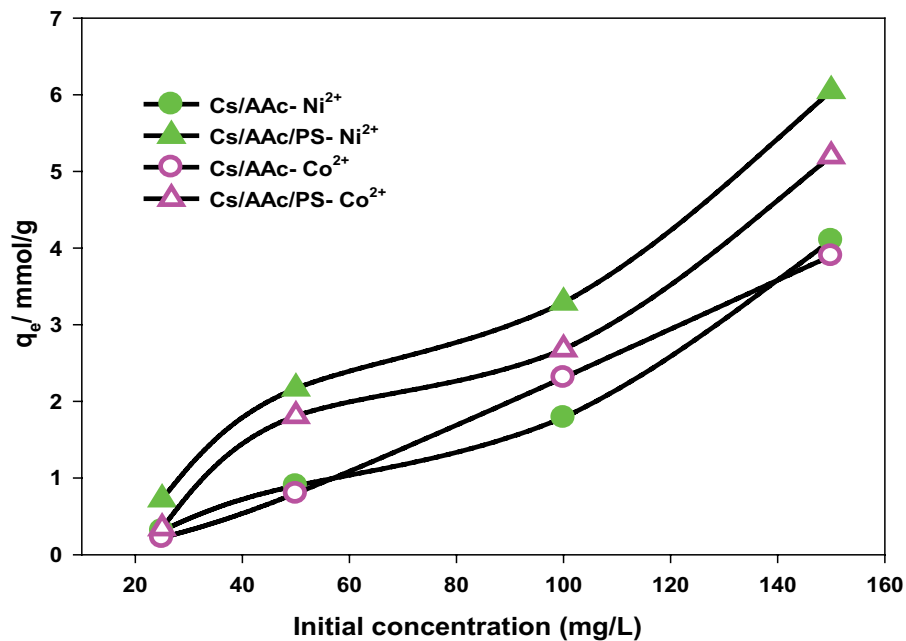


Fig. 7. Effect of initial concentration on the adsorption capacity of Co²⁺ and Ni²⁺ by 0.1 g of Cs/AAc/PS composite compared with Cs/AAc parent hydrogel in 25 mL at pH 6 and contact time 24 h.

radius of Ni²⁺ is 4.04 Å and for Co²⁺ is 4.23 Å. The smaller size of Ni²⁺ than Co²⁺ may be responsible for preferring its adsorption. Also, the electronegativity (Pauling scale) of cobalt (1.88) is lower than nickel (1.91) [34].

3.1.2. Effect of metal ion concentration

The adsorption capacity dependence on the initial concentration of Ni²⁺ and Co²⁺ by Cs/XN/AAc-PS and Cs/XN/

AAc sorbents is shown in Fig. 7. It can be noted that the adsorption capacity values increase with increasing the initial metal ion concentration from 25 to 150 mg/L. This indicated that the accessible adsorption sites on the adsorbents are sufficient for adsorption. Also, the increase in the initial metal ions concentration may accelerate the diffusion of Ni²⁺ and Co²⁺ ions into the polymeric networks due to increasing the driving force of the concentration gradient. The strong connection between the high number of

metal ions and the available adsorption sites increases the probability of the interaction between them [35]. The maximum q_e was found to be at initial concentration 150 mg/L that was 6.84 mmol/g for Ni²⁺ and 3.73 mmol/g for Co²⁺ ions. A comparison of the adsorption capacities of different adsorbing materials towards Ni²⁺ and Co²⁺ is obtained in Table 1.

3.1.3. Effect of adsorbent dosage

Fig. 8 represents the influence of Cs/XN/AAC-PS and Cs/XN/AAC sorbent dosages on the adsorption of Ni²⁺ and Co²⁺ ions. The results explained that as the adsorbent dosage increases, the sorption capacity values decrease. The maximum capacity was done at adsorbent dosage of 0.1 g. By extending the adsorbent dose, the active sites become higher than metal ions. Thus, a decrease in adsorption capacity was observed [43].

3.1.4. Effect of temperature

Fig. 9 shows the influence of temperature on the adsorption capacity of Ni²⁺ and Co²⁺ ions. It can be observed that the adsorption capacity increases as the temperature is increased where it recorded the maximum value at 60°C. The mobile species have sufficient energy to undergo interactions with active sites at the surface [44]. The results pointed to the adsorption reaction is endothermic.

3.1.5. Adsorption in the binary solution

The adsorption capacity of Cs/XN/AAC-PS and Cs/XN/AAC towards of Ni²⁺ and Co²⁺ ions in a binary solution to know the selectivity was done. Table 2 shows metal ions selectivity by 0.1 g of Cs/AAC and Cs/AAC/PS towards Ni²⁺ and Co²⁺ ions at pH 6 and initial metal ion concentration 20 mg/L for each metal ions. It can be observed that the selectivity towards Ni²⁺ is higher than Co²⁺ for both Cs/XN/

Table 1
The adsorption capacities of different adsorbing materials towards Ni²⁺ and Co²⁺. Comparison of adsorption Ni²⁺ and Co²⁺ onto Cs/AAC/PS nanocomposite with other hydrogels

Metal ions	Adsorbent	Adsorption capacity (mmol/g)	Reference
Ni ²⁺	Carboxymethyl cellulose hydrogel beads	4.06	[36]
	Chitosan	2.71	[37]
	Magnetic (2-acrylamido-2-methyl-1-propanesulfonic acid)	1.958	[38]
	Poly(N-hydroxymethyl acrylamide/2-hydroxyethyl acrylate)	0.739	[39]
	This study	6.84	
Co ²⁺	Modified PVC	3.45	[40]
	Zinc(II) doping chitosan/hydroxyapatite	1.9075	[41]
	Carboxylated sugarcane bagasse	0.800	[42]
	This study	3.73	

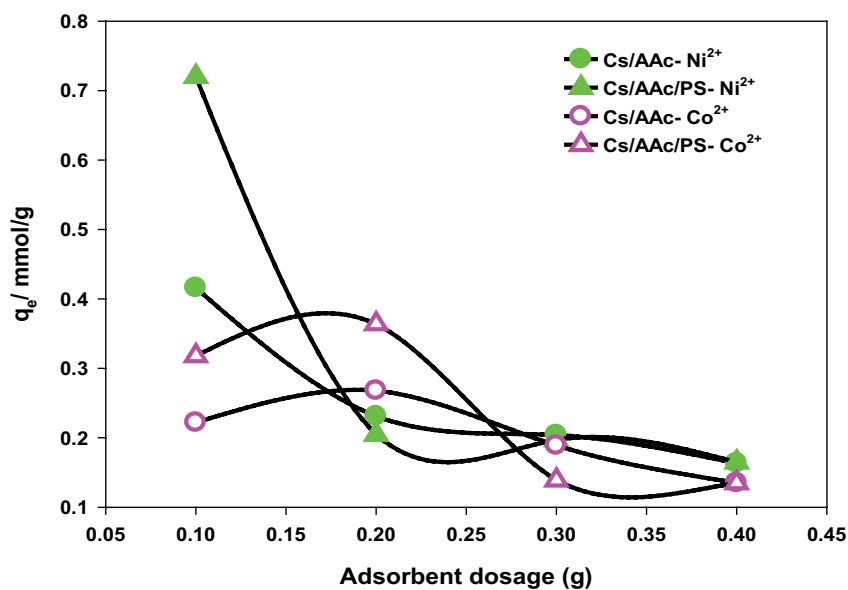


Fig. 8. Effect of adsorbent dosage on the adsorption capacity of Co²⁺ and Ni²⁺ by of Cs/AAC/PS composite compared with Cs/AAC parent hydrogel in 25 mL of initial concentration 20 mg/L at pH 6 and contact time 24 h.

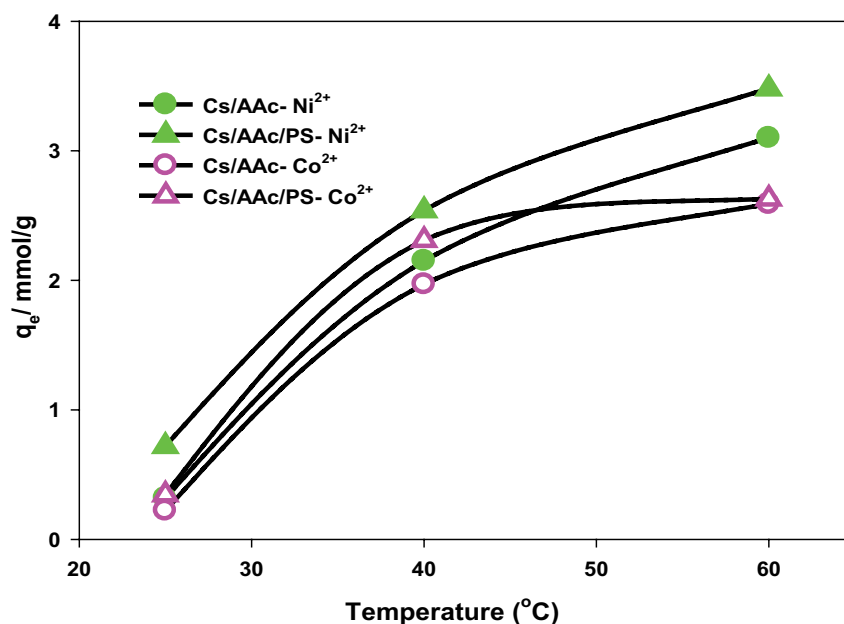


Fig. 9. Effect of temperature on the adsorption capacity of Co^{2+} and Ni^{2+} by 0.1 g of Cs/AAC/PS composite compared with Cs/AAC parent hydrogel in 25 mL of initial concentration 20 mg/L at pH 6 and contact time 24 h.

Table 2

Metal ions selectivity by 0.1 g of Cs/AAC and Cs/AAC/PS towards Ni^{2+} and Co^{2+} ions at pH; 6, treatment time; 24 h, initial metal ion concentration 20 mg/L for each metal ions of total volume 25 mL

Items	Ni^{2+}	Co^{2+}
Hydrated radius (Å)	4.04	4.23
(mmol/g)	0.8230	0.6418
Cs/AAC/PS (mmol/g)	2.4200	1.4360

AAC-PS and Cs/XN/AAC, The smaller hydrated radius of Ni^{2+} than Co^{2+} ions may be permit to more ions to be near the active sites on the adsorbent.

4. Conclusions

The Cs/XN/AAC-PS composite was successfully prepared in an aqueous medium using gamma irradiation technique performed via the free radical mechanism. The gel content was enhanced by increasing AAC content in the network matrix. According to the obtained data 10 kGy irradiation dose is sufficient to cross-link the network structure. It can be noted that the gel content increases with increasing the irradiation dose from 10 to 30 kGy however, a decrease in gel content was observed at raising the irradiation dose to 40 kGy. The swelling percentage was decreased by increasing AAC content and irradiation dose except at 40 kGy. The surface morphology investigation by FESEM confirmed that the surface was turned from a beehive structure into crushed by adding PS in Cs/XN/AAC-PS composite. DLS examination revealed that PS is ordinarily distributed, and the average size is 266 nm. The removal of Ni^{2+} and Co^{2+} from

aqueous solution by Cs/XN/AAC-PS composite was performed. The adsorption capacity improved with increasing pH from 3.0 to 6.0 where the maximum adsorption was done. The adsorption affinity towards Ni^{2+} is higher than Co^{2+} , and the maximum adsorption was done at 60°C. It can be noted that the adsorption capacity increases with increasing the initial metal ion concentration from 25 to 150 mg/L.

References

- [1] X. Wang, Y. Guo, L. Yang, M. Han, J. Zhao, X. Cheng, Nanomaterials as sorbents to remove heavy metal ions in wastewater treatment, *J. Environ. Anal. Toxicol.*, 2 (2012) 1–7, doi: 10.4172/2161-0525.1000154.
- [2] A.-F. Ngomsik, A. Bee, J.-M. Siaugue, D. Talbot, V. Cabuil, G. Cote, Co(II) removal by magnetic alginate beads containing Cyanex 272, *J. Hazard. Mater.*, 166 (2009) 1043–1049.
- [3] H. Hu, Z. Wang, L. Pan, Synthesis of monodisperse Fe_3O_4 @silica core-shell microspheres and their application for removal of heavy metal ions from water, *J. Alloys Compd.*, 492 (2010) 656–661.
- [4] S. Sharifi, R. Nabizadeh, B. Akbarpour, B. Akbarpour, A. Azari, H.R. Ghaffari, S. Nazmara, B. Mahmoudi, L. Shiri, M. Yousefi, Modeling and optimizing parameters affecting hexavalent chromium adsorption from aqueous solutions using Ti-XAD7 nanocomposite: RSM-CCD approach, kinetic, and isotherm studies, *J. Environ. Health Sci. Eng.*, 17 (2019) 873–888.
- [5] C. Femina Carolina, P. Senthil Kumar, A. Saravanan, G. Janet Joshiba, Mu. Naushad, Efficient techniques for the removal of toxic heavy metals from aquatic environment: a review, *J. Environ. Chem. Eng.*, 5 (2017) 2782–2799.
- [6] E.N. Zare, A. Motahari, M. Sillanpää, Nano-adsorbents based on conducting polymer nanocomposites with main focus on polyaniline and its derivatives for removal of heavy metal ions/dyes: a review, *Environ. Res.*, 162 (2018) 173–195.
- [7] M. Padervand, M.R. Gholami, Removal of toxic heavy metal ions from waste water by functionalized magnetic core-zeolitic shell nanocomposites as adsorbents, *Environ. Sci. Pollut. Res.*, 20 (2013) 3900–3909.

- [8] E.S. Abdel-Halim, S.S. Al-Deyab, Chemically modified cellulosic adsorbent for divalent cations removal from aqueous solutions, *Carbohydr. Polym.*, 87 (2012) 1863–1868.
- [9] Z. Li, Y. Wang, N. Wu, Q. Chen, K. Wu, Removal of heavy metal ions from wastewater by a novel HEA/AMPS copolymer hydrogel: preparation, characterization, and mechanism, *Environ. Sci. Pollut. Res.*, 20 (2013) 1511–1525.
- [10] Y.A. Zheng, D.J. Huang, A.Q. Wang, Chitosan-g-poly(acrylic acid) hydrogel with crosslinked polymeric networks for Ni²⁺ recovery, *Anal. Chim. Acta*, 687 (2012) 193–200.
- [11] H.V. Tran, L.D. Tran, T.N. Nguyen, Preparation of chitosan/magnetite composite beads and their application for removal of Pb(II) and Ni(II) from aqueous solution, *Mater. Sci. Eng., C*, 30 (2010) 304–310.
- [12] W. Zhang, F. Xu, Y. Wang, M. Luo, D. Wang, Facile control of zeolite NaA dispersion into xanthan gum–alginate binary biopolymer network in improving hybrid composites for adsorptive removal of Co²⁺ and Ni²⁺, *Chem. Eng. J.*, 255 (2014) 316–326.
- [13] G.A. Mahmoud, S.E. Abdel-Aal, N.A. Badway, S.A. Abo Farha, E.A. Alshafei, Radiation synthesis and characterization of starch-based hydrogels for removal of acid dye, *Starch/Stärke*, 66 (2013) 1–10, doi: 10.1002/star.201300117.
- [14] A. Afkhami, M. Saber-Tehrani, H. Bagheri, Simultaneous removal of heavy-metal ions in wastewater samples using nano-alumina modified with 2,4-dinitrophenylhydrazine, *J. Hazard. Mater.*, 181 (2010) 836–844.
- [15] D. Sud, G. Mahajan, M.P. Kaur, Agricultural waste material as potential adsorbent for sequestering heavy metal ions from aqueous solutions – a review, *Bioresour. Technol.*, 99 (2008) 6017–6027.
- [16] M. Ilyas, A. Ahmad, M. Saeed, Removal of Cr(VI) from aqueous solutions using peanut shell as adsorbent, *J. Chem. Soc. Pak.*, 35 (2013) 760–768.
- [17] R. Li, Y. Zhang, W. Chu, Z. Chen, J. Wang, Adsorptive removal of antibiotics from water using peanut shells from agricultural waste, *RSC Adv.*, 8 (2018) 13546–13555.
- [18] S. Boumchita, A. Lahrichi, Y. Benjelloun, S. Lairini, V. Nenov, F. Zerrouq, Application of peanut shell as a low-cost adsorbent for the removal of anionic dye from aqueous solutions, *J. Mater. Environ. Sci.*, 8 (2017) 2353–2364.
- [19] X.-K.O. Yang, L.-P. Yang, Z.-S. Wen, Adsorption of Pb(II) from solution using peanut shell as biosorbent in the presence of amino acid and sodium chloride, *BioResources*, 9 (2014) 2446–2458.
- [20] M.A. Abdel Khalek, G.A. Mahmoud, N.A. El-Kelesh, Synthesis and characterization of poly-methacrylic acid grafted chitosan-bentonite composite and its application for heavy metals recovery, *Chem. Mater. Res.*, 2 (2012) 1–12.
- [21] C. Dispenza, N. Grimaldi, M.A. Sabatino, I.L. Soroka, M. Jonsson, Radiation-engineered functional nanoparticles in aqueous systems, *J. Nanosci. Nanotechnol.*, 15 (2015) 3445–3467.
- [22] N. Grimaldi, M.A. Sabatino, G. Przybytniak, I. Kaluska, M.L. Bondi, D. Bulone, S. Alessi, G. Spadaro, C. Dispenza, High-energy radiation processing, a smart approach to obtain PVP-graft-AA nanogels, *Radiat. Phys. Chem.*, 94 (2014) 76–79.
- [23] C. Dispenza, M.A. Sabatino, N. Grimaldi, M.R. Mangione, M. Walo, E. Murugan, M. Jonsson, On the origin of functionalization in one-pot radiation synthesis of nanogels from aqueous polymer solutions, *RSC Adv.*, 6 (2016) 2582–2591.
- [24] J.M. Wasikiewicz, H. Mitomo, N. Nagasawa, T. Yagi, M. Tamada, F. Yoshii, Radiation crosslinking of biodegradable carboxymethylchitin and carboxymethylchitosan, *J. Appl. Polym. Sci.*, 102 (2006) 758–767.
- [25] S. Sultana, M. Rabiul Islam, N.C. Dafader, M.E. Haque, N. Nagasawa, M. Tamada, Effect of mono- and divalent salts on the properties of carboxymethyl cellulose hydrogel under irradiation technique, *Int. J. Chem. Sci.*, 10 (2012) 627–634.
- [26] M.F. Abou Taleb, G.A. Mahmoud, S.M. Elsigeny, E.-S.A. Hegazy, Adsorption and desorption of phosphate and nitrate ions using quaternary (polypropylene-g-N,N-dimethylamino ethylmethacrylate) graft copolymer, *J. Hazard. Mater.*, 159 (2008) 372–379.
- [27] S. Khan, N.M. Ranjha, Effect of degree of cross-linking on swelling and on drug release of low viscous chitosan/poly(vinyl alcohol) hydrogels, *Polym. Bull.*, 71 (2014) 2133–2158.
- [28] S.M. Fijul Kabir, P.P. Sikdar, B. Haque, M.A. Rahman Bhuiyan, A. Ali, M.N. Islam, Cellulose-based hydrogel materials: chemistry, properties and their prospective applications, *Prog. Biomater.*, 7 (2018) 153–174.
- [29] N. La, J. Dubey, P. Gaur, N. Verma, A. Verma, Chitosan based in situ forming polyelectrolyte complexes: a potential sustained drug delivery polymeric carrier for high dose drugs, *Mater. Sci. Eng., C*, 79 (2017) 491–498.
- [30] S. Faria, C.L. Oliveira Petkowicz, S.A.L. Morais, M.G. Hernandez Terrones, M.M. Resende, F.P. França, V.L. Cardoso, Characterization of xanthan gum produced from sugar cane broth, *Carbohydr. Polym.*, 86 (2011) 469–476.
- [31] N. Kulkarni, P. Wakte, J. Naik, Development of floating chitosan-xanthan beads for oral controlled release of glipizide, *Int. J. Pharm. Investig.*, 5 (2015) 73–80.
- [32] G.A. Mahmoud, A. Sayed, M. Thabit, G. Safwat, Chitosan biopolymer based nanocomposite hydrogels for removal of methylene blue dye, *SN Appl. Sci.*, 2 (2020) 968, doi: 10.1007/s42452-020-2753-9.
- [33] A. Hendy, E. Khozamy, G.A. Mahmoud, E. Saad, S. Serror, Implementation of carboxymethyl cellulose/acrylic acid/titanium dioxide nanocomposite hydrogel in remediation of Cd(II), Zn(II) and Pb(II) for water treatment application, *Egypt. J. Chem.*, 62 (2019) 1785–1798.
- [34] E.R. Nightingale Jr., Phenomenological theory of ion solvation. Effective radii of hydrated ions, *J. Chem. Phys.*, 63 (1959) 1381–1388.
- [35] G.A. Mahmoud, M.A. Abdel Khalek, E.M. Shoukry, M. Amin, A.H. Abdulghany, Removal of phosphate ions from wastewater by treated hydrogel based on chitosan, *Egypt. J. Chem.*, 62 (2019) 1537–1549.
- [36] S. Yang, S. Fu, H. Liu, Y. Zhou, X. Li, Hydrogel beads based on carboxymethyl cellulose for removal heavy metal ions, *J. Appl. Polym. Sci.*, 119 (2011) 1204–1210.
- [37] L. Pivarčiová, O. Rosskopfová, M. Galamboš, P. Rajec, Sorption of nickel on chitosan, *J. Radioanal. Nucl. Chem.*, 300 (2014) 361–366.
- [38] O. Ozay, S. Ekici, Y. Baran, N. Aktas, N. Sahiner, Removal of toxic metal ions with magnetic hydrogels, *Water Res.*, 43 (2009) 4403–4411.
- [39] Q. Zhu, Z. Li, Hydrogel-supported nanosized hydrous manganese dioxide: synthesis, characterization, and adsorption behavior study for Pb²⁺, Cu²⁺, Cd²⁺ and Ni²⁺ removal from water, *Chem. Eng. J.*, 281 (2015) 69–80.
- [40] D. Bekchanov, H. Kawakita, M. Mukhamediev, S. Khushvaktov, M. Juraev, Sorption of cobalt(II) and chromium(III) ions to nitrogen- and sulfur-containing polyampholyte on the basis of polyvinylchloride, *Polym. Adv. Technol.*, 32 (2021) 2700–2709.
- [41] C.P. Liu, Removal of cobalt(II) ions from aqueous solution on zinc(II) ions doping chitosan/hydroxyapatite composite, *Adv. Compos. Lett.*, 22 (2013), doi: 10.1177/096369351302200603.
- [42] A.L.P. Xavier, O.F.H. Adarme, L.M. Furtado, G.M.D. Ferreira, L.H.M. Silva, L.F. Gil, L.V.A. Gurgel, Modeling adsorption of copper(II), cobalt(II) and nickel(II) metal ions from aqueous solution onto a new carboxylated sugarcane bagasse. Part II: optimization of monocomponent fixed-bed column adsorption, *J. Colloid Interface Sci.*, 516 (2018) 431–445.
- [43] K.G. Akpomie, F.A. Dawodu, K.O. Adebowale, Mechanism on the sorption of heavy metals from binary-solution by a low cost montmorillonite and its desorption potential, *Alexandria Eng. J.*, 54 (2015) 757–767.
- [44] G.A. Mahmoud, S.E. Abdel-Aal, N.A. Badway, A.A. Elbayaa, D.F. Ahmed, A novel hydrogel based on agricultural waste for removal of hazardous dyes from aqueous solution and reuse process in a secondary adsorption, *Polym. Bull.*, 74 (2017) 337–358.